AD-A088 086 NAVAL RESEARCH LAB WASHINGTON DC F/G 18/1
ELECTRON CYCLOTRON/UPPER HYBRID RESONANT PREIONIZATION IN THE I--ETC(U)
UNCLASSIFIED JUN 80 R M GILGENBACH, R F LUCEY, K E HACKETT DOE-EX-77-A-34-1015
NRL-MR-4248 NL

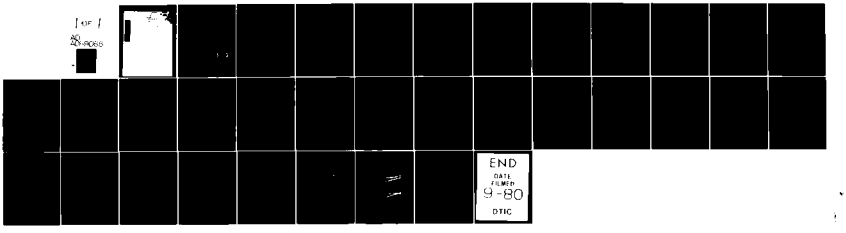

(14) NRL-MR-4248

(12) 34

SECURITY CLASSIFICATION OF THIS PAGE (When Data Entered)

(9) REPORT DOCUMENTATION PAGE

READ INSTRUCTIONS BEFORE COMPLETING FORM

1. REPORT NUMBER: NRL Memorandum Report 4248

2. GOVT ACCESSION NO.: AD-A088086

3. RECIPIENT'S CATALOG NUMBER:

4. TITLE (and Subtitle): ELECTRON CYCLOTRON/UPPER HYBRID RESONANT PREIONIZATION IN THE ISX-B TOKAMAK

5. TYPE OF REPORT & PERIOD COVERED: Interim report on a continuing NRL problem.

6. PERFORMING ORG. REPORT NUMBER:

7. AUTHOR(s): R.M. Gilgenbach, R.F. Lucey, K.E. Hackett, K.E. Burrell, M. Hacker, M.E. Read, V.L. Granatstein, A.C. England†, C.M. Loring†, J.B. Wilgen†, R. Isler†, Y-K.M. Peng†, A. Kulchar†, M. Murakami†, R. Richards†, O.C. Eldridge†† (Continues)

8. CONTRACT OR GRANT NUMBER(s): (15)

9. PERFORMING ORGANIZATION NAME AND ADDRESS: Naval Research Laboratory, Washington, D.C. 20375

10. PROGRAM ELEMENT, PROJECT, TASK AREA & WORK UNIT NUMBERS: 67-0865-0-0; DOE-EX-77-A-34-1015

11. CONTROLLING OFFICE NAME AND ADDRESS: Department of Energy, Washington, D.C. 20585

(11) 29

12. REPORT DATE: June 1980

13. NUMBER OF PAGES: 33

14. MONITORING AGENCY NAME & ADDRESS (if different from Controlling Office):

15. SECURITY CLASS. (of this report): UNCLASSIFIED

15a. DECLASSIFICATION/DOWNGRADING SCHEDULE:

16. DISTRIBUTION STATEMENT (of this Report)

Approved for public release; distribution unlimited.

17. DISTRIBUTION STATEMENT (of the abstract entered in Block 20, if different from Report)

DTIC ELECTE AUG 20 1980 S D B

18. SUPPLEMENTARY NOTES

19. KEY WORDS (Continue on reverse side if necessary and identify by block number)

Plasma heating
Tokamaks
Gyrotron
Electron cyclotron heatings

20. ABSTRACT (Continue on reverse side if necessary and identify by block number)

Preionization experiments have been performed on a tokamak by injecting about 80 kW of microwave power at 35 GHz for up to 15 ms. Microwave absorption occurs at the electron cyclotron and upper hybrid resonance frequencies as predicted by theory. Preionization causes substantial (40%) reductions in loop voltage during the initial phase of the tokamak shot. Flux (volt second) savings with preionization are about 30% in the first 2 ms or about 2% of the total flux expenditure in a tokamak shot. The plasma current starts 200 μs earlier and rises 1.4 times more rapidly in the preionized case. Electron densities of 5×10^{12} cm^{-3} can be sustained with only a toroidal magnetic field during microwave injection. The bulk electron temperature in the preionized plasma is about 10 eV although there are indications of higher electron temperatures (50 eV) in the upper hybrid resonance layer.

(Abstract continues)

DD FORM 1 JAN 73 1473 EDITION OF 1 NOV 65 IS OBSOLETE S/N 0102-LF-014-6601

25 1950 Jul

SECURITY CLASSIFICATION OF THIS PAGE (When Data Entered)

7. (Continued)

*JAYCOR, Alexandria, Virginia 22304
+Massachusetts Institute of Technology, Cambridge, Massachssetts 02139
**General Atomic Corporation, La Jolla, California 92037
Naval Research Laboratory, Washington, D.C. 20375
†Oak Ridge National Laboratory, Oak Ridge, Tennessee 37830
††University of Tennessee, Knoxville, Tennessee 38163

20. (Continued)

During the early stages of ohmic heating the preionization is effective in decreasing the peak of the radiated power.

CONTENTS

1. INTRODUCTION 1

2. EXPERIMENTAL CONFIGURATION 3

3. EXPERIMENTAL RESULTS 6

4. THEORETICAL ESTIMATES AND INTERPRETATION 12

4.1 Particle Balance in the Quasi-Steady Phase 12

4.2 Energy Balance in the Quasi-Steady Phase 13

4.3 The Interchange Instability 16

4.4 Other Time Scales 17

5. CONCLUSIONS AND DISCUSSION 21

ACKNOWLEDGEMENTS 23

REFERENCES 24

ELECTRON CYCLOTRON/UPPER HYBRID RESONANT PREIONIZATION IN THE ISX-B TOKAMAK

1. INTRODUCTION

Preionization has become an important concept in designing the next generation of large tokamaks. Theory [1] predicts substantial reductions of the loop voltage when a plasma is initiated and heated prior to the onset of toroidal voltage. The resultant decrease in poloidal field power supply requirements has been shown [1] to have a significant impact on the cost of a large tokamak such as the Engineering Test Facility (ETF). Savings in tokamak poloidal field transformer flux will also permit longer tokamak pulse lengths. Since preionization eliminates the requirement of a large voltage spike for breakdown, it would permit thicker vacuum vessel walls in future tokamaks, enhancing their ability to withstand plasma disruptions. With sufficient power, plasma preheating could cause more rapid 'burn-through" the impurity radiation barrier [2].

Typical tokamak start-up techniques now in use or being suggested, include growing the plasma from a small minor radius or applying a negative voltage spike immediately before the turnon of the forward toroidal voltage. A variety of preionization schemes have been proposed, including injection of neutral beams, relativistic electron beams [3], or microwaves [1]. Plasma heating with microwaves at the electron cyclotron resonant frequency or upper hybrid resonant frequency has been demonstrated in octupoles [4] and spherators [5] to be an effective technique for heating cold plasma. Recent developments [6] in gyrotron (electron cyclotron maser) technology have pro-

Manuscript submitted April 9, 1980

vided high power microwave sources at the high frequencies ($\gtrsim$ 28 GHz) required to perform electron cyclotron/upper hybrid resonant preionization and heating in tokamaks. These sources have the advantage that the same equipment may be used for both preionization and bulk heating.[7]

Previous preionization experiments injected short pulses ($\lesssim$ 2 ms) of (10-40 kW) microwaves into a toroidal field device [8], tokapole [9], or tokamak [10]. There is evidence in our experiments on the ISX-B tokamak that longer pulses ($\gtrsim$ 5 ms) are required to examine the "equilibrium" properties of the preionized plasma. In these experiments the injection of (80 kW) unpolarized microwaves for up to 15 ms have enabled us to perform more detailed preionization experiments which can be extrapolated to larger tokamaks.

2. EXPERIMENTAL CONFIGURATION

The ISX-B (Impurity Studies Experiment) tokamak is an iron core device with a major radius (R_o) of 93 cm and a minor radius (a) of 27 cm. The vertical limiter positions allow a plasma elongation ratio of about 2. This tokamak operates in a range of toroidal magnetic fields (10-15 kG) such that the electron cyclotron resonant surface, (at which the source frequency (f_g) is equal to the electron cyclotron frequency [f_c]), can be located at any major radius (R) which is desired. A typical tokamak shot is initiated by discharging a capacitor bank through inner and outer poloidal field windings. This capacitor bank charging voltage was held constant at 400 V in these experiments, thus the 8:1 turns ratio induces a maximum loop voltage of 50 V. The standard gas puff starts 50 ms prior to the toroidal voltage and provides a prefill pressure of about 10^{-4} torr.

The microwave source in these experiments was the NRL 35 GHz gyrotron oscillator [11] which generated 10-20 ms pulses at power levels of 100-150 kW. Microwave power was transmitted in the TE_{01} mode using (6 cm ID) oversize circular waveguide with about 1 dB attenuation. As depicted in Fig. 1, the microwaves were incident from the midplane of the high field side of the torus with an angle of injection 45^o from a major radius at the plasma edge. The antenna consisted of an open circular waveguide with a reflecting plate which radiated an equal mixture of the ordinary and extraordinary waves. Radiation not absorbed in a single pass could be reflected from the vacuum vessel walls back into the plasma after multiple passes, however, significant power could not be reflected directly back to the center of the plasma after one reflection because of the width of the antenna radiation pattern ($\pm$ 17^o).

A variety of diagnostics were used to measure the electron temperature of the preionized plasma in these experiments. A double Langmuir probe was located at the top center of the vacuum chamber, behind the plasma limiter. The probe ion saturation current was monitored over a series of 18 identical shots with varying probe bias to obtain a characteristic from which the electron temperature could be derived.

An electrostatic particle energy analyzer (PEA) probe was inserted into the plasma to measure the parallel electron temperature and ion saturation current. This probe is similar in design to one used previously in the DIVA tokamak[12]. In this probe the collector current was measured using a logarithmic amplifier, which produced a voltage that varied linearly with selector bias. The selector bias could be swept linearly in time, repetitively during the discharge; if the sweep time is short compared to the time scale over which plasma parameters vary, a set of electron temperatures at multiple discrete times during the discharge is obtained. Alternately, the bias could be held fixed during a discharge and varied from one discharge to the next. This allowed a complete time history of electron temperature at the PEA position to be obtained with a time resolution limited by shot-to-shot reproducibility and by fluctuations in the collected current. The PEA probe was mounted in a bellows-sealed, stepping-motor driven vacuum feedthrough, which allowed the probe to be inserted to various depths in the vacuum vessel or retracted past an isolation valve. The feedthrough was installed on a port located 30.5 cm above the machine midplane. The PEA probe traveled along a line inclined downwards from the horizontal at a 15^{o} angle, so that the probe moved closer to the midplane as it was inserted farther into the vessel.

A grazing incidence spectrometer measured the temporal evolution of the oxygen and iron impurity radiation. The electron temperature could be estimated from line radiation data using the RECYCLE code[13].

The line-average electron density was measured by two separate 150 GHz microwave interferometers. One of these interferometers measured the average electron density along a vertical chord at the center of the vacuum chamber (R_o= 93 cm), while the other measured the average density along a horizontal chord at the midplane of the tokamak.

A high speed (~3000 frames/s) movie camera was oriented to view the plasma horizontally, perpendicular to a major radius at the midplane of the tokamak. This permitted observation of the temporal behavior of the plasma in the breakdown stage and ohmic heating stage for both types of discharges, with and without microwave preionization.

3. EXPERIMENTAL RESULTS

Two categories of experiments were performed to determine the properties of the preionized plasma. In the first category, the "toroidal field only" shots, microwave power was injected into the tokamak with the normal gas filling pressure and the toroidal field (B_T), but no toroidal voltage was applied. The microwave pulses (80 kW) of 15 ms duration ionized the hydrogen in the vessel and produced a low-temperature, poorly-confined plasma with no toroidal current. This plasma was therefore similar to that produced in the second category of "preionization" experiments in which the microwaves were used to preionize the fill gas several milliseconds prior to the initiation of a tokamak discharge.

For the "toroidal field only" shots, the equivalent of a time resolved electron density profile was obtained by measuring the central line-average (l.a.) vertical density ($\bar{n}_v$) and varying the toroidal magnetic field from shot-to-shot. These results, given in Fig. 2, demonstrate that a low density plasma ($\omega_c \simeq \omega_{uH}$), is produced 1 ms after the beginning ($\tau = 0$) of the microwave pulse. The peak density is apparently located at the cyclotron resonance (B_T = 12.5 kG). At τ = 2 ms the peak density apparently moves toward a lower magnetic field, indicating absorption at the upper hybrid resonance. This is confirmed by high speed movies which show that the plasma forms in a narrow resonant layer during the first millisecond and subsequently broadens toward the lower magnetic fields. This behavior is in agreement with theory, which predicts that the plasma is initiated in a resonant vertical layer at $\omega = \omega_c$ then spreads to a location where $\omega = \omega_{uH}$ as the density increases. The interchange instability and $\underline{E} \times \underline{B}$ drift also cause plasma convection toward lower magnetic fields. If one assumes from Figure 2 that the upper hybrid resonance occurs at a magnetic field of 11.2 kG with a source frequency

($\omega_g = \omega_{uH}$) of 35 GHz, the corresponding density is calculated to be $\sim 3 \times 10^{12}$ cm^{-3}, in good agreement with the line-average densities of Figure 2. High speed movies show that after about 5 ms, the plasma attains a configuration determined by the antenna radiation pattern and confined between the electron cyclotron resonance and the outer vacuum vessel wall. This configuration appears to remain quiescent for the last 10 ms of a 15 ms microwave pulse. In these "toroidal field only" experiments, the electron density decays to half its value about 10 ms after the microwaves are turned off. This particle confinement time indicates that the bulk of the plasma electrons are rather cold ($T_e \approx 10$ eV).

The-line average horizontal density ($\bar{n}_{eH}$) and vertical density interferometer signals are given in Figures 3(a) and (b) respectively for tokamak shots without and with preionization. Microwaves were injected from t = - 9 ms to t = + 2 ms, (where t = 0 corresponds to the onset of the plasma current). For the typical base pressure of 10^{-4} torr the electron density saturated approximately 4 ms after the start of the microwave pulse. With a higher gas puff rate the density increased to $\sim 5 \times 10^{12}$ cm^{-3} throughout a 15 ms microwave pulse. Decreasing the gas puff rate caused the density to saturate more rapidly at the lower value of 2×10^{12} cm^{-3}. This suggests that preionization could permit tokamak startup over a wide range of initial densities.

Prior to the application of toroidal current, the plasma is vertically elongated by a factor of 2, corresponding to the vertical limiter positions. This explains why $\bar{n}_{ev}$ appears greater than $\bar{n}_{eH}$ in Fig. 3(b). After the onset of plasma current, the density increases more gradually in the preionized case, but saturates at the same value after the plasma current reaches its steady state value. Magnetic pickup loops give some indication that the pre-

ionized plasma may be more stable in the first 10 ms of the toroidal current rise.

Typical oscillographs of the loop voltage, electron density, and plasma current are given in Figure 4 during the first 2 ms of the tokamak shot. The large voltage spike in Figure 4(a) is a transient effect since the loop voltage is limited to 50 V by the 8:1 reduction of the 400 V capacitor bank. At 400 μs the loop voltage without preionization is 50 V compared to 30 V when preionizing microwaves were injected from t = - 7 ms to + 2 ms. The voltseconds saved in the first 2 ms amount to 0.01 V sec or about 30% of the total expenditure during that period. One expects the difference in V_ℓ at 2 ms to be small since the ohmic heating power at this time is about 200 kW compared to 80 kW of microwave power. With higher microwave power it should be possible to realize savings in loop voltage which persist to later times in the discharge. Preheating by more than 1 ms prior to the application of toroidal voltage produced no further decrease in loop voltage, indicating that the energy confinement time of the preionized plasma is short ($\lesssim$ 1 ms).

The plasma current is driven by mutual induction from a capacitor bank discharge through a saturable reactor connected in series with the poloidal field windings. Although the capacitor bank charging voltage was constant in these experiments, the decay of the capacitor bank current (I_c) was delayed in tokamak shots with preionization. This accounts for the lower loop voltage (V_ℓ) with preionization since

$$\frac{M\, dI_c}{dt} = I_p R + L_p \frac{dI_p}{dt} \qquad (1)$$

where M is the mutual inductance between the poloidal field windings and the plasma, R is the plasma resistance, and L_p is the total plasma inductance (internal and external).

From Fig. 4, it is apparent that the plasma current starts at t = 0 in the preionized case, whereas the current rise is delayed by 200 μs in the standard breakdown. This 200 μs current delay represents transformer flux which is expended in breaking down the fill gas in a standard tokamak discharge. The microwave plasma breakdown thus produces a further volt-second savings from this term. The rate of current rise was 1.4 times more rapid when preionization was applied, presumably due to the lower resistive component of the loop voltage.

The effect of ECH/UHR preheating on spectral radiation during the early phase of the discharge is illustrated in Fig. 5. The preionization microwave pulse is initiated 7 ms before the ohmic current starts (t = 0) and has a duration of 9 ms. O II and O III are readily produced during this time. The peaks of the radiation from stages O II - O VI are noticeably lower than the levels observed when ohmic heating alone is employed. Similar results are observed in iron, at least through the stage Fe XIV, and the pyroelectric detector which serves as a total radiometer verifies that the power losses immediately following the start up of the ohmic current are reduced. This reduction of radiative losses clearly leads to conservation of transformer volt-seconds.

The electron temperature resulting from preionization can be estimated from the data of Figure 5. These estimates are made from the RECYCLE Code [13] which is not explicitly time dependent. However, it does allow one to follow the excitation and ionization of particles moving into plasmas with increasing temperature gradients and, hence, is implicitly time dependent. From Figure 5 it is observed that O II is very near its peak intensity 6 or 7 ms after the preionization pulse is turned on; the line average electron concentration is $3.8 \times 10^{12}/cm^3$ at this time. Computations indicate that if the confinement time is very long ($\tau >> 10$ ms) this line should reach a

maximum when T_e 10 eV. However, the oxygen radiation appears to reach a steady state in 5-10 ms and if this period is assumed to represent the confinement time, T_e is calculated to be 11 - 13 eV due to the microwave pulse.

The electron temperature of the preionized plasma with only a toroidal field was measured by the Langmuir probe and the particle energy analyzer. During the microwave pulse the Langmuir probe current was eratic and could not be interpreted. The probe characteristic immediately after the microwave pulse indicated an electron temperature of 8 eV ($\pm$ 2 eV) behind the limiter.

Electron temperature data from the PEA were obtained at t = 11 msec (after the start of ECH), at three positions. Here the toroidal magnetic field on axis was about 13 kG, thus the ω_{ce} layer was located at R_c = 96 cm and the ω_{uH} layer would be at the major radius R_{uH} = 108 cm. At R = 110 cm (i.e., 2 cm outboard of the ω_{uH} layer) the parallel electron temperature was 45 eV $\pm$ 5 eV. Just inside of the ω_{uH} layer, at R = 106 cm, a temperature of 50 eV $\pm$ 5 eV was measured at t = 11 msec. However, the temperature between the ω_{ce} layer and the ω_{uH} layer (R = 101 cm), at t = 14 msec, was found to be only 8.4 $\pm$ 0.8 eV.

The PEA data are consistent with the following picture of the evolution of the plasma during the ECH pulse. At the onset of ECH, the chamber is rapidly (within 1 msec) filled with a uniform, low density, low-temperature plasma, except for a thin layer of hotter, denser plasma localized near the ω_{ce} layer. Later in the ECH pulse, the overall electron density increases, and the high-density, high-temperature layer moves radially outwards, following the upper hybrid resonance layer as the electron density increases. Late in the discharge, then, the PEA will see the low-temperature "background" plasma away from the ω_{uH} layer, but will see higher temperature at larger

radii because it is closer to the upper hybrid layer. The time dependence of the saturation current for a stationary probe located outboard of the ω_{ce} layer would also have the observed qualitative form. If the localized layer of hot, dense plasma is sufficiently thin, then spectroscopic temperature measurements, which are line-averaged, will yield a low electron temperature, more characteristic of the background plasma than of the hot layer. This also appears consistent with observations.

Thomson scattering measurements of electron temperature during the current rise phase indicate a higher electron temperature for the preionized discharges. One could explain this in terms of both the slower rate of density rise (Fig. 3) and the more rapid rate of current rise (Fig. 4) when preionization was employed.

For the range of gas pressures in these preionization experiments we observed no significant change in the hard X-ray flux from runaway electrons. Both the preionized and standard discharges exhibited hard X-rays only at the end of the pulse.

It was possible to initiate discharges with lower poloidal field capacitor bank voltage both with and without preionization. It appeared, however, that when the capacitor bank voltage was lower the ohmic heating power was insufficient to break through the radiation barrier. This resulted in a condition where the entire transformer flux was expended in the burnout phase of the discharge.

4. THEORETICAL ESTIMATES AND INTERPRETATION

The experimental results just presented contain several features that should be discussed more fully. These include: (1) the energy balance for the quasi-steady phase of the discharge, a quiescent plasma with $n_e \lesssim 5(10)^{12}$ cm^{-3}, $T_e \cong 10$ eV and possibly higher ($T_e \cong 50$ eV) near the upper hybrid resonance (UHR); (2) the anomalously fast plasma convection early in the RF pulse, which is probably caused by the interchange instability; (3) the effective absorption of the RF power by the plasma with indications of enhanced absorption at the UHR.

4.1 Particle Balance in the Quasi-Steady Phase.

The plasma parameters are by and large consistent with the assumptions used in Ref. 1, while the particular case considered there assumed 120 kW of only extraordinary wave to lead to an estimated T_e of about 10 eV throughout the chamber and about 200 eV within a 2 cm thick UHR layer. Assuming that the enhanced absorption at the UHR is limited to the extraordinary mode, T_e there in the present experiment is expected to be significantly less than 200 eV with about 40 kW in the extraordinary mode.

If we suspend questions about the stability of the plasma in the absence of toroidal plasma current, an estimate of plasma parameters can be obtained based on relatively straightforward particle and energy balance considerations.

The electron density is determined by a balance between loss through curvature drift and gain from ionization. The curvature drift should dominate in a region free from significant poloidal "stray" field (~ 1 gauss). In ISX-B this region is estimated to be roughly 50 cm by 30 cm around the center of the chamber. We have for nearly steady state:

$$n_e n_o S_H - n_e/\tau_{De} = 0 \qquad (2)$$

where

$$\tau_{De} = 5 \times 10^{-9}\ bRB/T_e \quad ,$$

S_H is the net ionization rate coefficient, b = 25 cm and the cgs units are used except eV is used for T. Equation (2) determines only the neutral density (n_o) as a function of T_e. The values of n_o for T_e = 10 eV, 50 eV and 100 eV are listed in Table A. It is seen that n_o depends only weakly on T_e. So with sufficient electron heating, n_e is determined essentially by the prefill pressure. A density of $n_e \sim 3 \times 10^{12}$ cm^{-3} corresponds to a pressure around 10^{-4} torr, which is consistent with the initial amount of gas puff.

4.2 Energy Balance in the Quasi-Steady Phase.

Ions form a channel of energy loss via electron-ion collisional transfer. An estimate of ion temperature (T_i) is needed before assessing the electron energy balance. We have approximately

$$Q_{ie} = \frac{3M_e}{M_i} \frac{n_e(T_e - T_i)}{\tau_{ie}} = \frac{3}{2} n \left[(T_i - T_e)\, n_o S_{cx} + \frac{T_i}{\tau_{Di}} \right] , \qquad (3)$$

assuming that the heating of the ions by collision with the electrons is balanced by charge exchange and curvature drift losses. For $n_e = 3 \times 10^{12}$ cm^{-3}, Eq. (3) provides an estimate of T_i as listed in Table A. It is seen that $T_i \sim T_e$ at low T_e($\sim$10 eV) while $T_i << T_e$ at high T_e ($\sim$ 100 eV). This is apparently due to the large increase of τ_{ie} with increasing T_e.

Table A. Estimated Values of N_o, T_i, and the Required RF Heating Power Density P_μ for T_e = 10, 50, and 100 eV and $n_e = 3 \times 10^{12}$ cm^{-3}

T_e(eV)	10	50	100
$n_o(cm^{-3})$	1.1×10^{10}	1.3×10^{10}	2.2×10^{10}
T_i(eV)	9.7	22	14
$P_\mu \left(\frac{erg}{cm^3 sec}\right)$ ($\eta = 0$)	2.3×10^4	2.3×10^5	6.4×10^5
$P_\mu \left(\frac{erg}{cm^3 sec}\right)$ ($\eta = 0.02$)	3.8×10^5	2.4×10^5	6.4×10^5

The energy balance for the electrons can be approximated by,

$$P_\mu = W_{ion}\, n_e n_o S_H + Q_{ie} + \frac{3}{2}\, n_e T_e/\tau_{De} + P_{rad}, \qquad (4)$$

where the RF heating power (P_μ) is balanced by losses due to ionization, collision with ions, curvature drift and impurity radiation (P_{rad}). Assuming an oxygen content of a few percent ($\eta = n_z/n_e \lesssim 0.02$), Eq. (4) shows that P_{rad} dominates when T_e = 10 eV, giving an estimate of P_μ as (see, Table A)

$$P_\mu \simeq (2.3 \times 10^4 + 1.8 \times 10^7 \times \eta)\ \text{erg/cm}^3\ \text{sec} \quad . \qquad (5)$$

This shows that the electron energy balance would be dominated by minute amounts of low-Z impurities. For a chamber volume of about 3×10^6 cm^3 and an RF power of 80 kW, Eq. (5) suggests an oxygen content of $\eta \simeq 1.4\%$.

For $T_e \sim 50$ eV to 100 eV, Eq. (4) shows that the electron energy balance would be dominated by loss due to curvature drift and also influenced significantly by ionization and electron-ion collisions if impurity content remains at a few percent. The requirement in P_μ is then estimated to be $2.4 - 6.4 \times 10^5$ erg/cm^3 sec. The estimated RF power deposited within a 4-cm layer at the UHR is then 3 kW to 8 kW, respectively. A reduction in η by 0.1% in the bulk plasma would provide the surplus RF power to heat the UHR electrons to 50-100 eV.

It is seen that the available data on the RF heated plasma seem consistent with the implications of Eq. (4). Measurements of T_i and n_z are needed to help determine whether T_e in the UHR layer is in the 50-100 eV range.

4.3 The Interchange Instability.

When a fraction f_μ of microwave power (P_μ = 80 kW) is absorbed in a volume V_p = 3 m^3, with an average electron density $\bar{n}_e = 5 \times 10^{12}$ cm^{-3}, the heating rate of each electron is

$$\frac{d\bar{W}}{dt} = \frac{f_\mu P_\mu}{\bar{n}_e V_p} = f_\mu \, 3.3 \times 10^4 \text{ eV/sec.} \qquad (6)$$

The observed electron energy $\bar{W} = 3T_e/2 = 15$ eV gives an energy containment time $\tau_E = 0.45 \text{ msec}/f_\mu$. This time can be accounted for by a small concentration of impurities emitting line radiation.

Theoretically, the microwave energy should be deposited in a much smaller volume, producing a higher heating rate and a higher temperature. The impurity radiation would then be much smaller. The interchange instability [14] is probably responsible for the fast convection. The interchange of two tubes of flux that are loaded with plasma is energetically favorable for instability on the outboard side of the tokamak, where the field lines curve away from the plasma. The mechanism for the instability is the short wavelength polarization field produced by the curvature and field gradient drifts [15]. The growth rate is

$$\gamma = V_s[k/R]^{1/2} = [T(eV)/\lambda(cm)]^{1/2} \, 3.3 \times 10^5 \text{ sec}^{-1} \qquad (7)$$

where V_s is the sound velocity and $k = 2\pi/\lambda$ is the wave number of the plasma perturbation, which is constant along magnetic field lines. In normal tokamak operation the toroidal current produces a rotational transform that stabilizes this mode. It may also be stable with a sufficiently gentle pressure gradient [1].

4.4 Other Time Scales.

The electron drift from the magnetic field gradient is vertical with a time scale,

$$\tau_M = \frac{m\omega_{ce}Rb}{2T_e} = \frac{290 \text{ msec}}{T_e(eV)} \quad , \tag{8}$$

where b = 50 cm is the half-height of the chamber. Electrons and ions drift at the same rate in opposite directions. When a charge displacement occurs, a macroscopic electric field develops and both species drift outward together in a time

$$\tau_D = \frac{aB}{Ec} = \frac{110 \text{ msec}}{V(\text{volts})} \quad , \tag{9}$$

where V is the potential and a = 27 cm is the half width.

The motion pictures show that some plasma reaches the top of the machine at the cyclotron resonant surface within a fraction of a millisecond. A few electrons may be heated to kilovolt temperatures very early in the pulse, drifting quickly to the wall.

Ionization by electron impact occurs in a time

$$\tau_i = \frac{1}{n_o < \sigma v >_i} \quad , \tag{10}$$

with a minimum at an electron temperature of T_e = 70 eV of $\tau_i(\text{min})$ = 3.7 μsec for $n_o = 1 \times 10^{13}$ cm^{-3}. About 35 eV per electron is required for ionization, with most of the energy lost through line radiation. This time increases as $T_e^{\frac{1}{2}}$ for higher temperature. Electrons travel along field lines around the machine in a time

$$\tau_c = 2\pi R(m/T_e)^{1/2} = \frac{13.9 \text{ μsec}}{[T_e(eV)]^{1/2}} \quad , \tag{11}$$

so an electron makes a few toroidal orbits for each ionizing collision.

The electron distribution becomes isotropic on a time scale

$$\tau_{ee} = 16.3 \text{ nsec } T_e(\text{eV})^{3/2} , \tag{12}$$

at the observed density, so it remains isotropic during ionization and heating. As a consequence of these time scales the plasma should be spread uniformly about the torus with no local density maximum near the antenna.

If an electron encounters a field error during each toroidal circuit, one expects the orbit to be displaced and expects a random walk out to the wall. For a step length δ one expects a random walk time

$$\tau_R = \left(\frac{a}{2\delta}\right)^2 \tau_c = \frac{3.2 \text{ msec}}{[\delta(\text{cm})]^2 [T_e(\text{eV})]^{1/2}} . \tag{13}$$

This time and the other containment times do not seem short enough to account for the energy loss. These mechanisms do account for the 10 msec decay time of the afterglow plasma in the experiments with toroidal field only.

4.5 Electron Heating.

Early in the RF pulse one expects linear cyclotron damping to completely absorb the microwave power. For very low electron density the plasma dispersion is ignorable and the fraction of microwave power absorbed is

$$f = 1 - \exp(-\eta) \tag{14}$$

where the optical depth is

$$\eta = 2\pi^2 \alpha R/\lambda , \tag{15}$$

with $\alpha = \omega_{pe}^2/\omega_{ce}^2$, and where λ is the free space wavelength. The theory is applicable when $\alpha < (2\pi T/mc^2)^{\frac{1}{2}} \cos\theta$. Total absorption occurs when $n_e > 2 \times 10^{10}$ cm^{-3}. The heating occurs in a small volume of width $\Delta = R \cos\theta \, T_e/mc^2 \,^{\frac{1}{2}}$, determined by the Doppler shift. From either the wave damping or from particle orbits [16] one finds a local heating rate for an average electron

$$\frac{d\bar{W}}{dt} = 2\pi \frac{e^2}{mc^2} \frac{P}{A} \frac{R\lambda}{\Delta\sqrt{2\pi}} \, e^{-x^2/2\Delta^2} = 2.8 \times 10^{10} \text{ eV/sec} \, \frac{e^{-x^2/2\Delta^2}}{\Delta(\text{cm})} \quad ,$$

when P = 80 kW, A = 1000 cm^2 is the area irradiated, and x is the distance from the resonant surface. The perpendicular energy gained is rapidly made isotropic and rapidly spread over the entire drift surface. This large heating rate is enough to explain the early vertical drift.

As the density increases the plasma dispersion must be included. One finds [12,13] an optical depth for the extraordinary wave:

$$\eta \cong \pi^2 \frac{T_e}{mc^2} \frac{R}{\lambda} \frac{\cos^2\theta}{\alpha} (2-\alpha)^{3/2}(1+\alpha)^2 \quad ,$$

for θ close to 90°. For the ordinary wave one finds

$$\eta \cong \pi^2 \frac{T_e}{mc^2} \frac{R}{\lambda} \alpha(1-\alpha)^{\frac{1}{2}} \quad .$$

For the parameters of this experiment this theory is applicable for $n_e > 1.2 \times 10^{11}$ cm^{-3}. The factor of T_e/mc^2 appears because both waves are left circularly polarized at cyclotron resonance and absorption depends on the Doppler shift.

The cyclotron absorption of the extraordinary wave is predicted to be complete when $n_e = 1 \times 10^{11}$ cm^{-3}, and to decrease to 9% with $n_e = 5 \times 10^{12}$ cm^{-3} for the temperature observed. Since the waves are launched from the high field side of the tokamak, at the higher density the extraordinary wave propagates to the upper hybrid resonance layer. There it may be absorbed in a nonlinear way or may turn back in the manner first discussed by Stix [19]. The absorption mechanisms are treated in Ref. 1. In any case, the absorption is predicted to be very efficient.

The absorption of the ordinary wave is very small in this density regime. The ordinary mode must be reflected and partially depolarized at the wall before it is absorbed. This multiple pass absorption may still be very efficient since the toroidal chamber has a high quality factor.

The upper hybrid resonance surface at $\omega = \omega_{uh} = (\omega_{pe}^2 + \omega_{pe}^2)^{\frac{1}{2}}$ is displaced toward the outer wall of the tokamak. The actual position of the layer depends on the density profile, and the microwave interferometer measures the density along fixed vertical and horizontal chords. In the later stages of the discharge the upper hybrid layer may well lie close to the outer wall, and the electron heating zone may be close to the wall, with a small energy containment time.

5. CONCLUSIONS AND DISCUSSION

These experiments have demonstrated that substantial (40%) reductions in loop voltage are obtained in the initial phase of a tokamak discharge when the plasma is preheated by microwaves at the electron cyclotron/upper hybrid resonance frequency. The flux saving from preionization is about 30% of the flux in the first 2 ms or 2% of the total volt-seconds expended in a tokamak shot. A large voltage is not required to cause breakdown when preionization is employed. If these results scale to larger tokamaks (e.g., ETF) they could significantly reduce the poloidal field power supply requirements, also permitting thicker vacuum vessel walls and longer tokamak shots.

Preionization eliminates a 200 μs delay in plasma current rise, thereby saving the transformer flux normally expended in breaking down the prefill gas. The lower resistive component of loop voltage causes the plasma current to rise 1.4 times more rapidly with preionization. Thus, the plasma could burn-through the impurity radiation barrier more rapidly.

Preionized plasma densities of 2-5 x 10^{12} cm^{-3} typically exist with particle confinement times of about 10 ms when microwaves are injected with only a toroidal magnetic field. The microwave absorption is at the electron cyclotron frequency for low densities, but as the density increases the absorption occurs at the upper hybrid resonance frequency. The preionized plasma appears to attain a stable configuration defined by the antenna radiation pattern between the electron cyclotron resonance and the outer wall. The apparent stability of the plasma presents an intriguing subject of investigation.

Electron temperatures in the bulk of the plasma have been measured to be 8-13 eV, however, there are indications that electron temperatures in the upper hybrid layer may be as high as 50 eV. The low electron temperatures (10 eV) agree with other experiments of this type [10], but are much lower than the peak temperature predicted theoretically. A possible explanation is that other loss mechanisms are present and that higher temperature electrons are produced only at the upper hybrid resonance region.

ACKNOWLEDGEMENTS

We gratefully acknowledge the support of J. Sheffield and the entire ISX-B tokamak group, especially M. J. Saltmarsh, H. E. Ketterer, S. C. Bates, C. E. Bush, J. L. Dunlap, R. Dyer, T. C. Jernigan, J. Lyons, G. H. Neilson, V. K. Pare, and D. Swain. We also thank S. Borowski, and W. M. Mannheimer for useful discussions.

This work was supported by the Office of Fusion Energy, U.S. Department of Energy under the following contracts: (i) Contract No. EX-77-A-34-1015 with the Naval Research Laboratory; (ii) Contract No. W-7405-ENG-26 with the Union Carbide Corporation; (iii) Contract No. ET-78-S-02-4714 with the Massachusetts Institute of Technology.

REFERENCES

1. Y-k. M. Peng, S. K. Borowski, and T. Kammish, Nucl. Fusion 18 (1978) 1489.

2. R. J. Hawryluk and J. A. Schmidt, Nucl. Fusion 16 (1976) 775.

3. A. Mohri, International Atomic Energy Agency, CN-37-X.

4. J. C. Sprott, Phys. Fluids 14 (1971) 1795.

5. M. Okabayashi, K. Chen, and M. Porkolab, Phys. Rev. Lett. 31, 1113 (1973).

6. V. A. Flyagin, et al., IEEE Trans. Microwave Theory Tech. 25, 514 (1977); J. L. Hirschfield and V. L. Granatstein, IEEE Trans. Microwave Theory Tech. 25, (1977) 522.

7. R. M. Gilgenbach et al. Phys. Rev. Lett. 44 (1980) 647.

8. A. I. Anisomov, N. I. Vinogradov, B. P. Poloskin, Sov. Phys. Tech. Phys. 18 (1973) 459; 20, (1976) 626; 20 (1976) 629.

9. D. F. Holly, D. F. Witherspoon, J. C. Sprott, Bull. Am. Phys. Soc. 23, 878 (1978).

10. D. G. Bulyginsky, M. M. Larionov, L. S. Levin, O. V. Miklukho, A. I. Tokunov, and N. V. Shustova, Report #611 from Ioffe Physical Institute (1979).

11. M. E. Read, R. M. Gilgenbach, R. Lucey, K. R. Chu, and V. L. Granatstein, IEEE Transactions on Microwave Theory and Techniques (to be published).

12. H. Kimura et al., Nuclear Fusion 18 (1978) 1195.

13. ONRL Technical Memorandum.

14. J. D. Callen, private communication.

15. M. N. Rosenbluth and C. L. Longmire, Ann. Phys. 1, 120 (1957).

16. O. C. Eldridge, Phys. Fluids 15, 676 (1972).

17. A. G. Litvak, G. V. Permitin, E. V. Suvorov, A. A. Frajaman, Nucl. Fusion 17, 654 (1977).

18. O. C. Eldridge, W. Namkung, A. C. England, ORNL/TM-6052, Oak Ridge National Laboratory (Nov. 1977) submitted to Nuclear Fusion.

19. T. H. Stix, Phys. Rev. Lett. 15, 878 (1965).

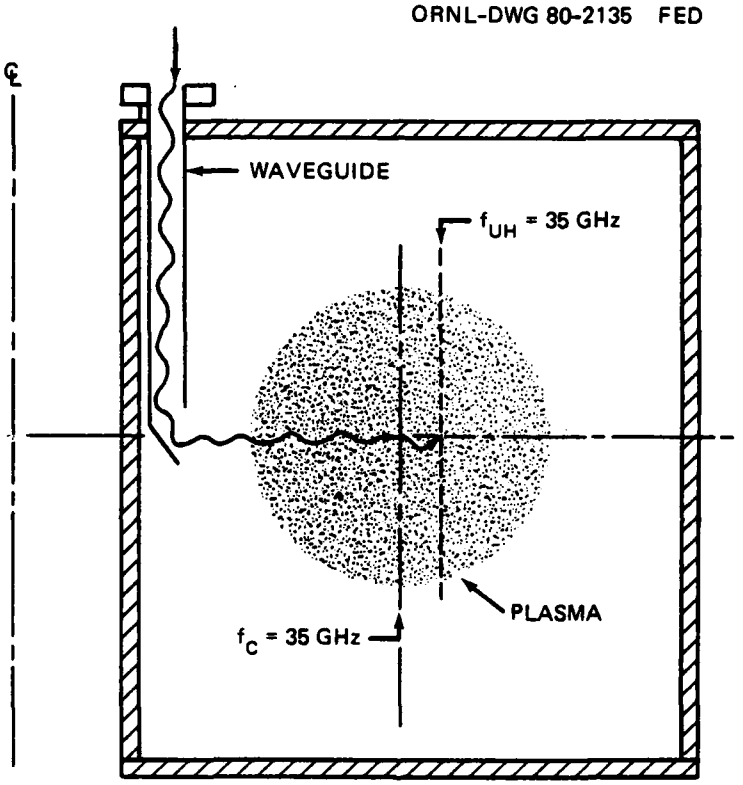

Fig. 1 — Experimental configuration. Unpolarized microwaves are launched from a reflecting plate antenna located on the high field side of the torus. The location of the electron cyclotron resonant surface (f_c = 35 GHz) and upper hybrid resonant surface (f_{uH}= 35 GHz) are shown for a toroidal magnetic field on axis B_T = 12.5 kG and an electron density of 3 x 10^{12} cm^{-3}.

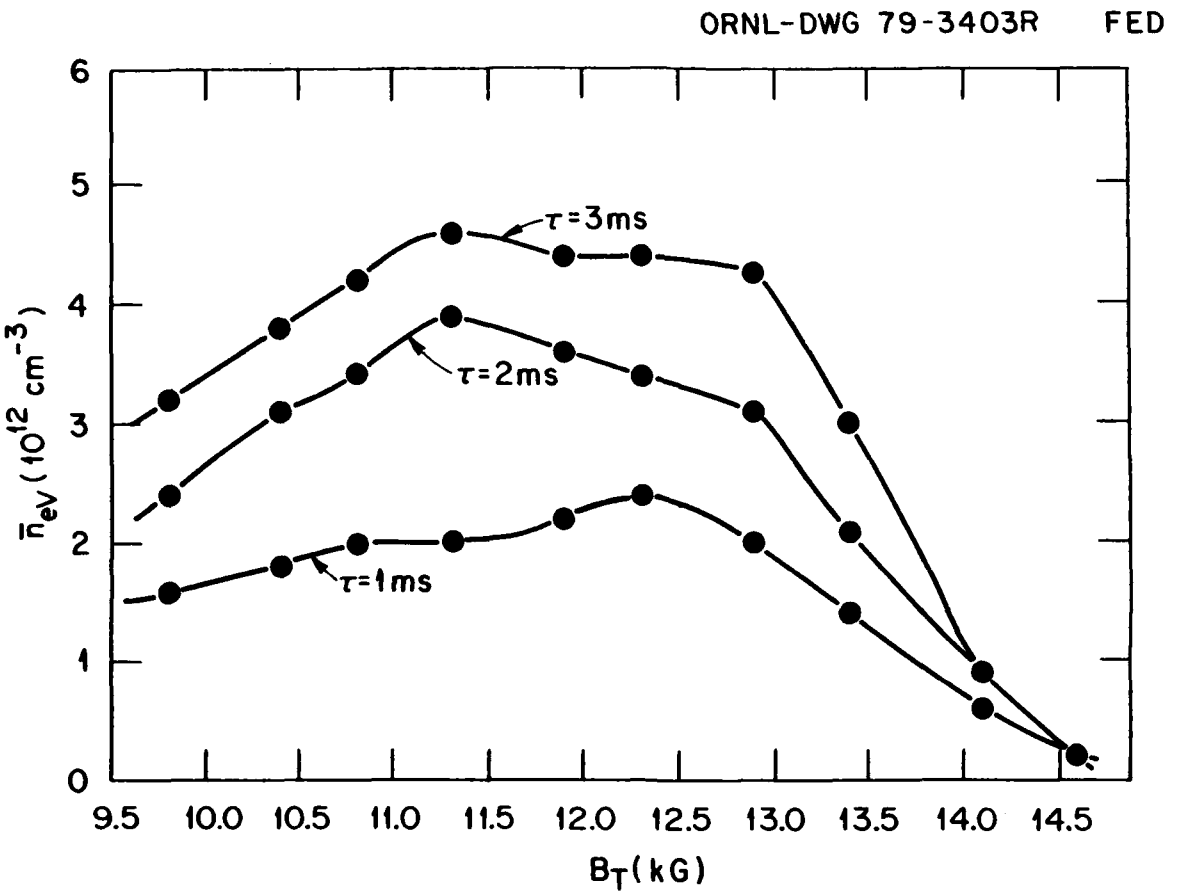

Fig. 2— Line average electron density measured through a vertical chord at the center of the vacuum vessel. By varying the toroidal magnetic field from shot-to-shot the equivalent of a time resolved density profile is obtained.

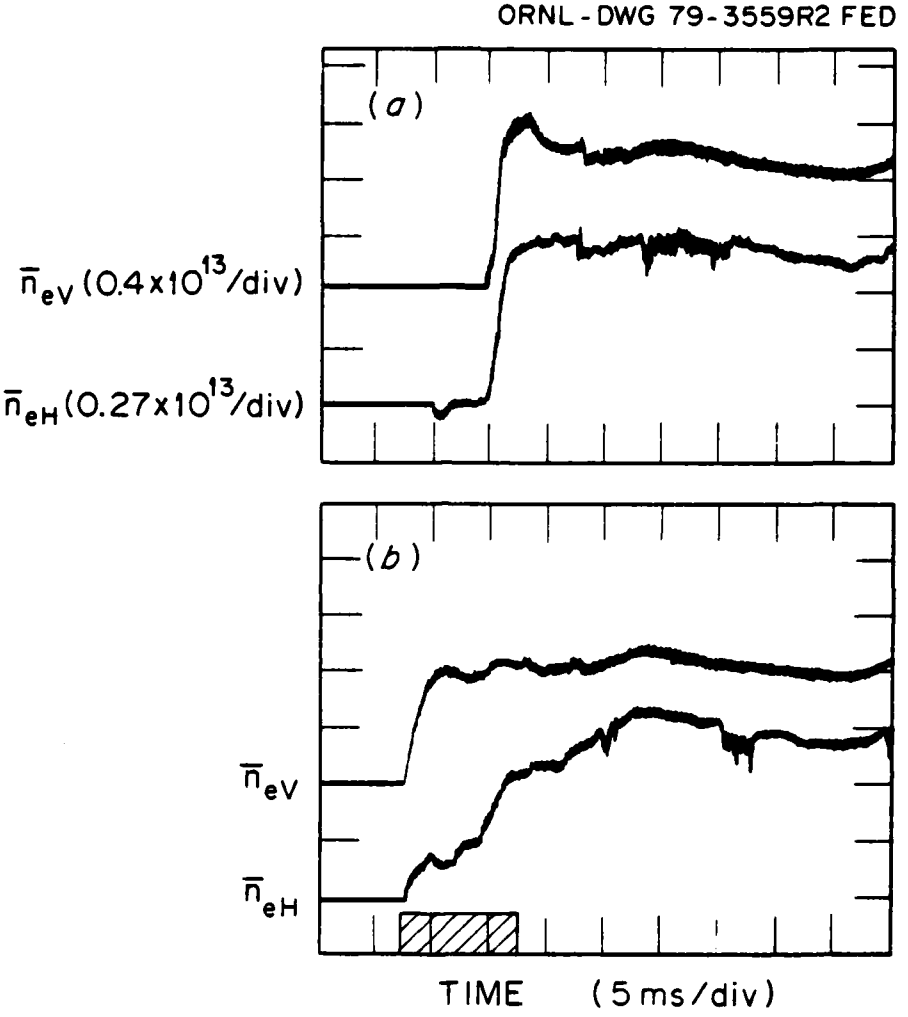

Fig. 3 — Temporal evolution of the line-average electron density measured vertically ($\bar{n}_{eV}$) and horizontally ($\bar{n}_{eH}$) for conditions: (a) standard tokamak discharge without preionization, and (b) tokamak discharge with preionizing microwaves injected from t = -7 ms to t = +2 ms.

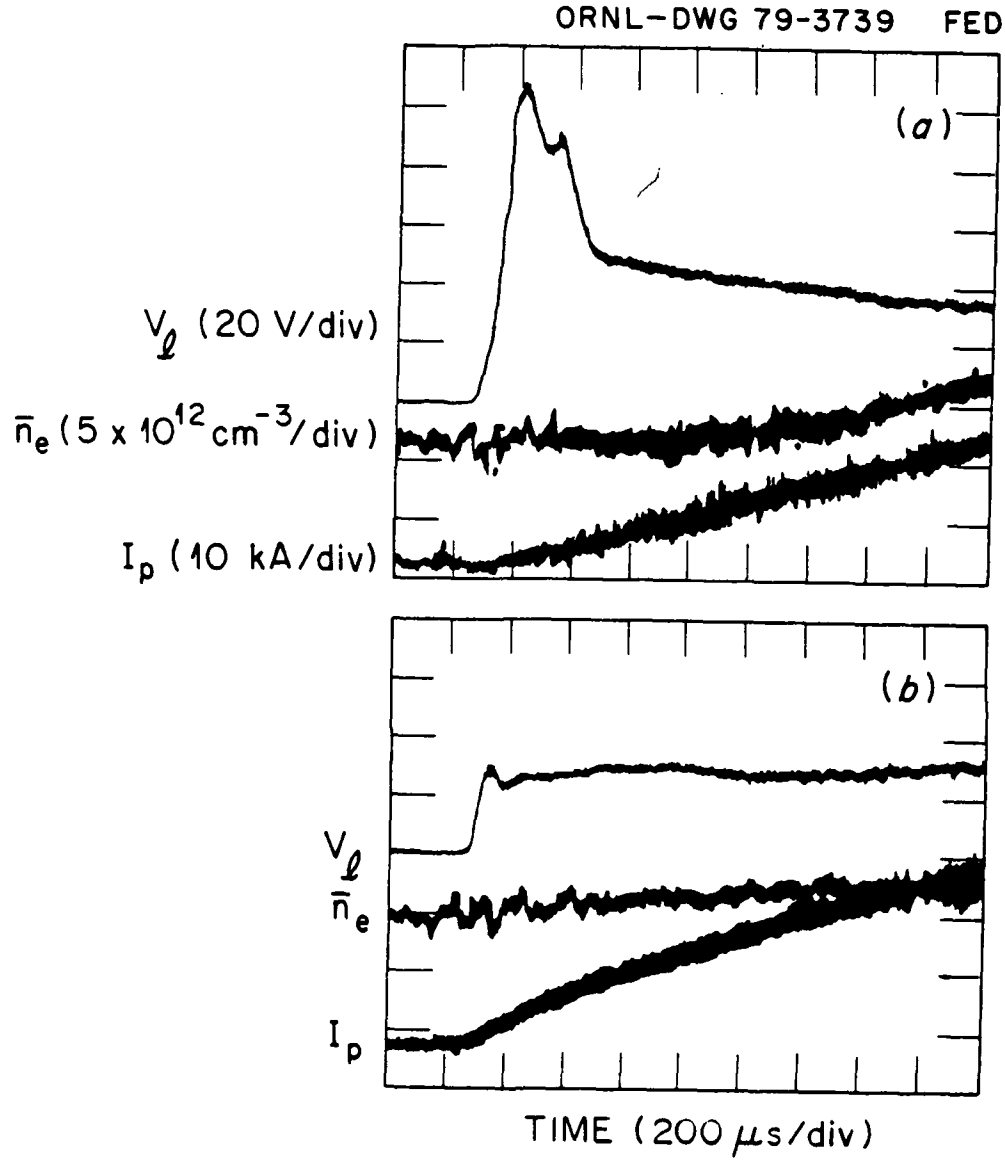

Fig. 4 — Temporal evolution of the loop voltage (V_ℓ), horizontal line-average electron density ($\bar{n}_e$), and plasma current (I_p) for conditions; (a) standard tokamak discharge without preionization and, (b) tokamak discharge with 80 kW preionizing microwaves injected from t = -7 ms to t = +2 ms.

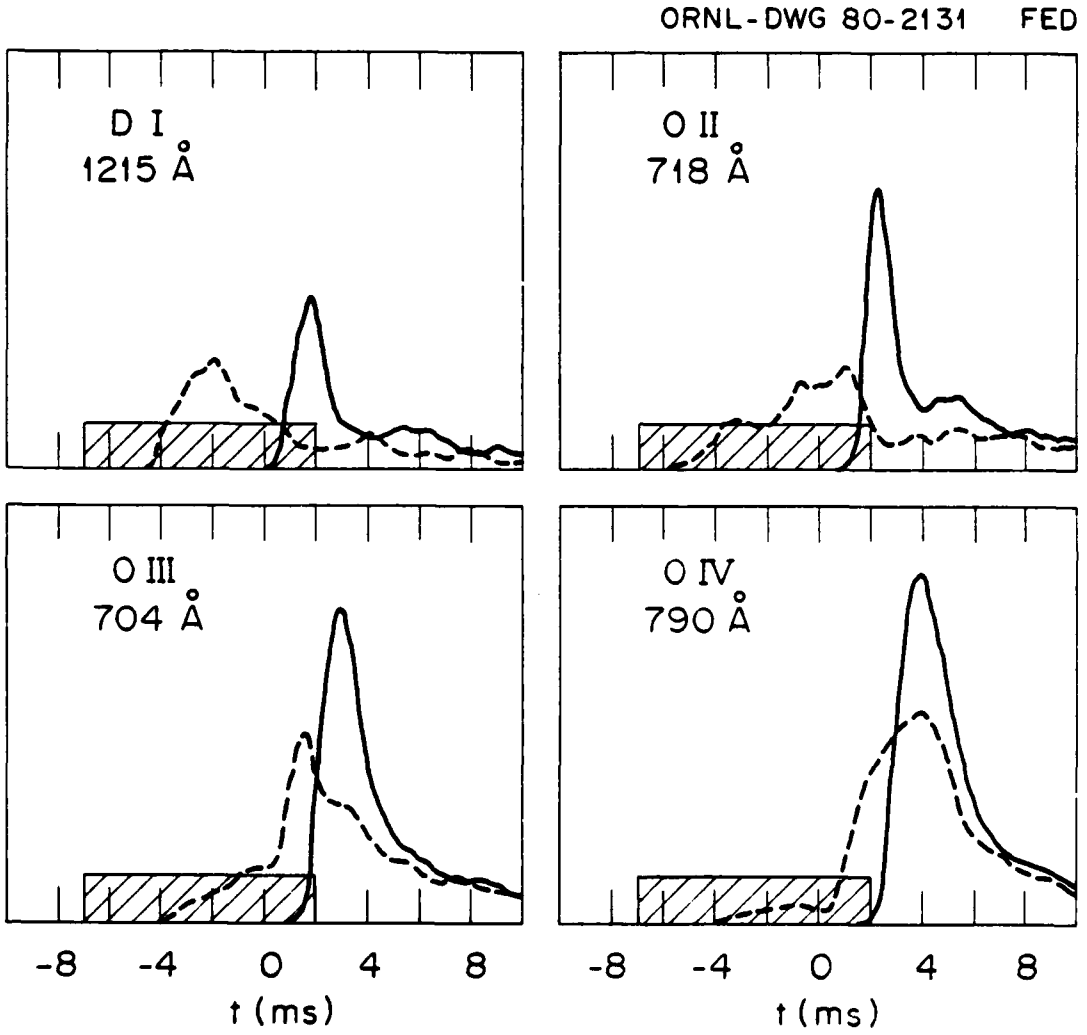

Fig. 5 — Spectral radiation measured by grazing incidence spectrometer. The solid lines denote data taken during standard tokamak discharge without preionization. Dashed lines denote data taken during tokamak discharge with 80 kW microwaves injected at times indicated by cross-hatched areas.